

# Higher-order mode analysis for SOLEIL-type superconducting cavity

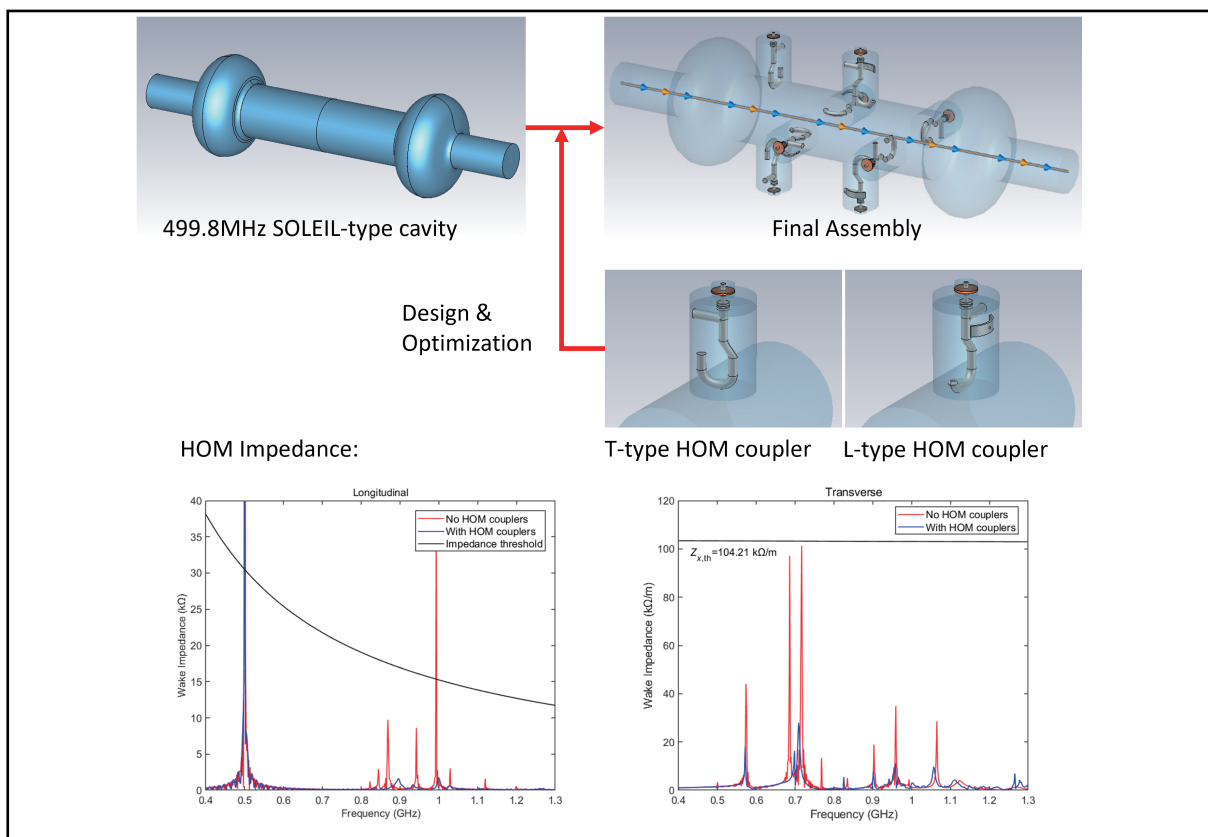
Xiyuan Chai, Qin Li, Yunpeng Xu, Yungai Tang, Mingsheng Tan, and Cong-Feng Wu

National Synchrotron Radiation Laboratory, University of Science and Technology of China, Hefei 230029, China

Correspondence: Cong-Feng Wu, E-mail: [cfwu@ustc.edu.cn](mailto:cfwu@ustc.edu.cn)

© 2024 The Author(s). This is an open access article under the CC BY-NC-ND 4.0 license (<http://creativecommons.org/licenses/by-nc-nd/4.0/>).

## Graphical abstract




## Public summary

- The 499.8 MHz SOLEIL-type superconducting cavity and its higher-order mode (HOM) couplers were designed for the first time in this paper.
- The HOM damping requirements of Hefei Advanced Light Facility (HALF) were satisfied for both longitudinal and transverse impedances, and the effect of asymmetry on transverse impedance was observed.
- HOM couplers were analyzed and optimized for radio frequency transmission, multipacting, and thermal calculations. No thermal breakdown is induced until the multipacting effect occurs.

# Higher-order mode analysis for SOLEIL-type superconducting cavity

Xiyuan Chai, Qin Li, Yunpeng Xu, Yungai Tang, Mingsheng Tan, and Cong-Feng Wu 

National Synchrotron Radiation Laboratory, University of Science and Technology of China, Hefei 230029, China

 Correspondence: Cong-Feng Wu, E-mail: [cfwu@ustc.edu.cn](mailto:cfwu@ustc.edu.cn)

© 2024 The Author(s). This is an open access article under the CC BY-NC-ND 4.0 license (<http://creativecommons.org/licenses/by-nc-nd/4.0/>).



Cite This: *JUSTC*, 2024, 54(7): 0706 (10pp)



Read Online

**Abstract:** A 499.8 MHz SOLEIL-type superconducting cavity was simulated and designed for the first time in this paper. The higher-order mode (HOM) properties of the cavity were investigated. Two kinds of coaxial HOM couplers were designed. Using 4 L-type and 4 T-type HOM couplers, the longitudinal impedance was suppressed to 3 k $\Omega$ , and the transverse impedance below 30 k $\Omega$ /m. The HOM damping requirements of Hefei Advanced Light Facility (HALF) were satisfied. This paper conducts an in-depth study on the radio frequency (RF) design, multipacting optimization, and thermal analysis of these coaxial couplers. Simulation results indicated that under operating acceleration voltage, the optimized couplers does not exhibit multiplying or thermal breakdown phenomena. The cavity has the potential to reach a higher acceleration gradient.

**Keywords:** HOM coupler; superconducting cavity; RF system; multipacting; thermal simulation

**CLC number:** TL54+4

**Document code:** A

## 1 Introduction

Synchrotron radiation light sources have become important devices for scientific research. As a main part of the accelerator radio frequency (RF) system, which provides energy to electrons, superconducting cavities have been widely used in the last 50 years because of their low ohmic power loss<sup>[1,2]</sup>. The SOLEIL-type cavity was named because it was first used in the 3rd generation light source SOLEIL<sup>[3]</sup>. Two 352.2 MHz SOLEIL-type superconducting modulators were installed on its storage ring in 2006 and 2008. They provided an accelerating voltage of 3 MV (750 kV/cell) and satisfied the power requirement for a beam current of 500 mA at a beam energy of 2.75 GeV<sup>[4]</sup>. Currently, SOLEIL cavities have the potential to operate under 500 mA beam current using a single cryomodule with some improvements in their solid-state power amplifiers (SSPAs)<sup>[5]</sup>.

The Hefei Advanced Light Facility (HALF), a large-scale scientific apparatus in the 14th five-year development plan of China, is a soft X-ray and VUV light source based on a diffraction-limited storage ring (DLSR), which has a beam energy of 2.2 GeV and an emittance goal of less than 100 pm-rad. It is now under construction at the National Synchrotron Radiation Laboratory (NSRL). Based on KEK-B<sup>[6]</sup> and BEPC-II<sup>[7]</sup>, a KEK-type superconducting cavity has been developed and will be used in HALF to meet the 350 mA beam current requirement<sup>[8]</sup>. In the future, with the increasement of beam current and number of insert parts, exploring SOLEIL-type superconducting cavities, which have two fundamental power couplers, may be meaningful. The linear section length of a 499.8 MHz SOLEIL module with two fundamental

power couplers may be shorter than that of the two KEK modules because a higher power level could be easily realized.

All modes except the fundamental mode that exist in the cavity are called higher-order modes (HOMs). HOMs are excited when relativistic electrons passing through the cavity and must be extracted efficiently to prevent coupled bunch instability (CBI). HOM damping concepts may vary but are principally based on coaxial and waveguide couplers as well as beam line absorbers or any combination<sup>[9]</sup>. SOLEIL-type superconducting cavities were equipped with coaxial HOM couplers on their center pipe to reduce the linear section length and to have a moderate opening at the end beam pipes. Four HOM couplers were mounted on a 352 MHz SOLEIL cavity to extract the HOMs. Six HOM couplers were used to meet the HOM damping requirement of a 1500 MHz SUPER3HC 3rd harmonic cavity<sup>[10]</sup>.

In this paper, the finite element analysis software CST Suite Studio was used to complete the research. First, the HOM properties of a bare 499.8 MHz SOLEIL-type superconducting cavity were analyzed. Second, coaxial HOM couplers were assumed to act as hooks to optimize their quantity and location, which has a great influence on the multipacting analysis. Then, the RF transmission properties and multipacting properties of the HOM couplers were optimized. Fourth, detailed HOM couplers were added to the model for the confirmation of the design and for overall optimization. Finally, a primary thermal simulation was presented to explore the cooling requirements of HOM couplers.

**Table 1.** Main parameters for the 499.8 MHz SOLEIL-type superconducting cavity

Parameter	Value
$R_{SBP}$	91.5 mm
$R_{eq}$	269.4 mm
$R_{CBP}$	141.0 mm
$L_{left}$	151.5 mm
$L_{right}$	151.5 mm
$a_{11}$	24.4 mm
$b_{11}$	33.1 mm
$a_{12}$	130.5 mm
$b_{12}$	130.5 mm
$a_{r1}$	30.8 mm
$b_{r1}$	52.6 mm
$a_{r2}$	112.5 mm
$b_{r2}$	112.5 mm
$L_{CBP}$	912 mm
$f_0$	499.785 MHz
$R/Q$ (for each cell)	44.289 $\Omega$
geometrical factor	297.290 $\Omega$
$E_{peak}/E_{acc}$	1.77
$B_{peak}/E_{acc}$	4.26 mT/(mV•m)

## Materials and methods

### 1 Cavity analysis

A 499.8 MHz SOLEIL-type superconducting cavity was analyzed by CST Suite Studio based on the 352 MHz SOLEIL cavity. The main parameters are listed in Table 1.

As shown in Fig. 1, the SOLEIL-type cavity have cells linked with a large beam pipe in between, called the center beam pipe (CBP), and terminated on smaller side beam pipes (SBPs). The radius of the CBP was specially designed to ensure that all the HOMs could be extracted into the CBP while the fundamental mode was still localized in cavity cells. When HOM couplers were assembled on CBP, this structure provided strong coupling to HOMs and very weak coupling to the fundamental mode.

Theoretically, HOMs between the fundamental mode frequency  $f_0$  and the cutoff frequency of the SBP  $f_{c,SBP}$  should be extracted by coaxial HOM couplers on the CBP. HOMs with frequencies above  $f_{c,SBP}$  were assumed to be absorbed at the beam pipe absorbers or lossy metal tapers assembled outside the crymodule. In our case, as the radius of the SBP was set to 91.5 mm, the cutoff frequency was calculated to be 965.95 MHz in  $TE_{11}$  and 1261.87 MHz in  $TM_{01}$ . Therefore, HOMs with frequencies between 499.8 MHz and 1261.87 MHz are of particular concern.

To find HOMs that may have a strong effect on the beam, the wake impedance is an accurate and convenient approach<sup>[11,12]</sup>. It can be calculated by 2D software such as ABCI or 3D software such as the wakefield solver in CST Particle Studio. Using the cavity model in Fig. 1, two SBP ports were set as waveguide ports with five modes. The beam was set at a 1 mm bias from the cavity center, parallel to the red line in Fig. 1, and had a 34 mm bunch length. The wavelenght was set to 800 m. The wake impedance was calculated and is shown in Fig. 2. The peak at approximately 499.8 MHz represented the fundamental mode, and the other peaks represented HOMs that may be dangerous. For HOMs that have a higher frequency, the electromagnetic field modes in the cavity cell and CBP may be different. They were named EM (frequency in MHz). For example, mode  $EM_{(716)}$  has a field similar to that of  $TM_{111}$  in cavity cells, while the distribution in CBP is  $TE_{112}$ . All HOM impedances were notably high and will be further increased with increasing simulation wavelenght. This phenomenon can be attributed to the absence of HOM couplers in the model depicted in Fig. 1, which allows the HOMs to sustain resonance within the cavity.

### 2 Cavity analysis with HOM coupler hooks

According to the coupling method, coaxial-type HOM couplers can be divided into two categories, probe couplers or loop couplers, using electrical coupling or magnetic coupling, respectively<sup>[13]</sup>. Since the loop coupler could be designed to be dismountable and sometimes easier to use to form a filter structure, it was chosen as the basis for our HOM couplers.

#### 2.1 Impedance threshold

The wake impedance threshold to cause CBI should not be exceed both longitudinal and transverse. It can be analytic-

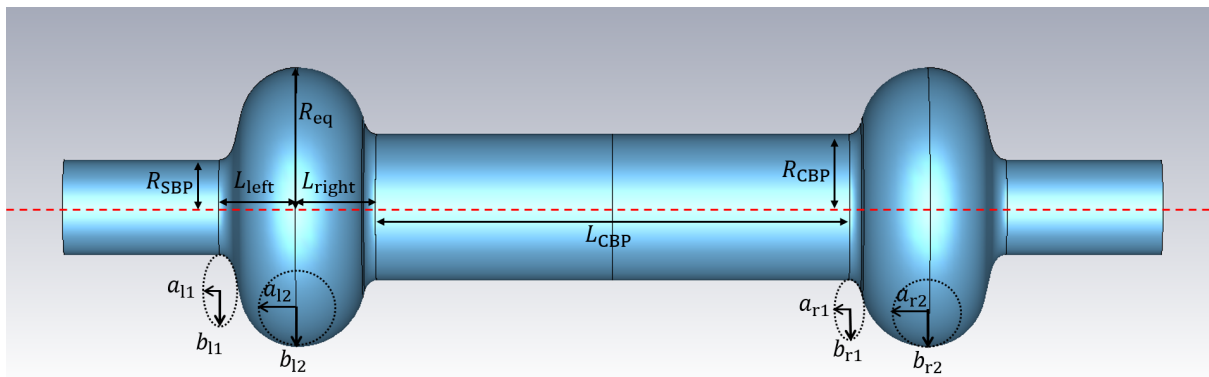


**Fig. 1.** 499.8 MHz SOLEIL-type superconducting cavity.

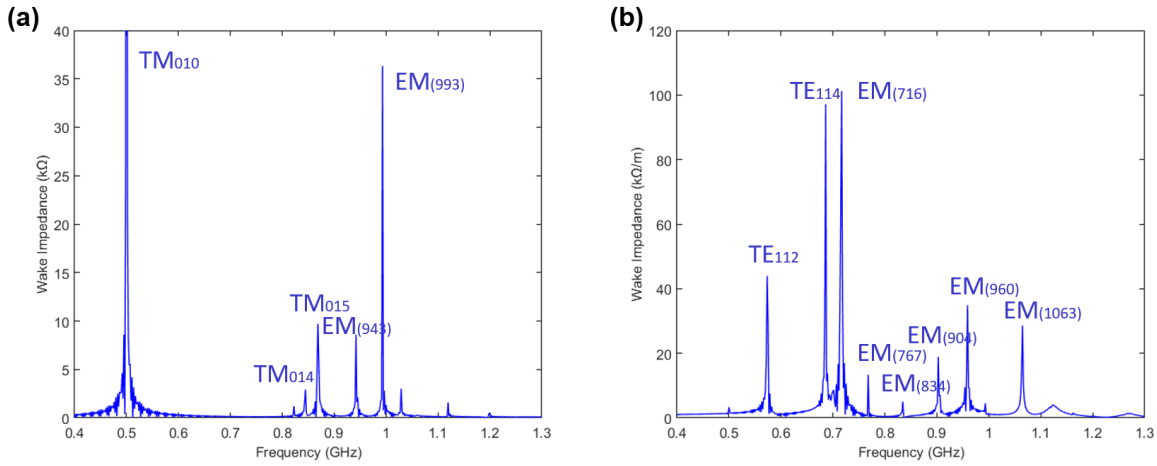


**Fig. 2.** Wake impedance calculation results for a bare 499.8 MHz SOLEIL-type superconducting cavity: (a) longitudinal and (b) transverse

ally calculated with the widely used Eqs. (1) and (2)<sup>[3,9]</sup>.

$$f_{\text{HOM}} Z_{\parallel}^{\text{th}} = \frac{2Q_s E}{\alpha \tau_{\parallel} I_0}, \quad (1)$$

$$f_0 Z_{\perp}^{\text{th}} = \frac{2E}{\beta_{\perp} \tau_{\perp} I_0}, \quad (2)$$

where  $f_{\text{HOM}}$  and  $f_0$  are the HOM resonance frequency and revolution frequency,  $E$  and  $I_0$  are the beam energy and average current,  $Q_s$  is the synchrotron tune,  $\alpha$  is the momentum compaction factor,  $\beta_{\perp}$  is the  $\beta$  function at the cavity location in the  $x$  or  $y$  direction, and  $\tau_{\parallel}$  and  $\tau_{\perp}$  are the longitudinal and transverse radiation damping times, respectively. These formulas were obtained by equating the radiation damping time with the respective instability rise time.

## 2.2 Coupler quantity and location

To achieve strong coupling, the plane of the hook should be as perpendicular as possible to the magnetic field line and close to the strong field. As shown in Fig. 3, the magnetic field of transverse HOMs such as  $TE_{112}$  tends to localize around the cavity, and longitudinal HOMs such as  $TM_{015}$  have a strong field around the center of the CBP. In our pre-

diction, two kinds of couplers were needed: T-type couplers with hooks perpendicular to the beam axis and close to the cells, as shown in Fig. 3a, and L-type couplers parallel to the beam axis and mounted around the center of the CBP, as shown in Fig. 3b, which handle transverse and longitudinal HOMs, respectively.

To estimate the quantity of HOM couplers and their location, couplers were assumed to be hooks added to the cavity model. Otherwise, the large mesh number and unacceptable calculation time will make the optimization impossible. A model with 4 T-type and 2 L-type couplers is shown in Fig. 4; L-type couplers are located around the center, and T-type couplers are located near the cavity cell. Couplers with different orientations were considered to absorb transverse HOMs with different polarizations.

We used the CST wakefield solver to optimize the model. During the optimization, the number of couplers and the distance between the couplers and cavity were varied to obtain a smaller impedance. All coupler ports were set as waveguide ports with TEM mode, and two SBP ports were set as waveguide ports with five modes. The beam was set to a 1 mm offset from the axis, and a long simulation wavelenght of 1000 m was used to ensure that all the HOMs were extracted. A

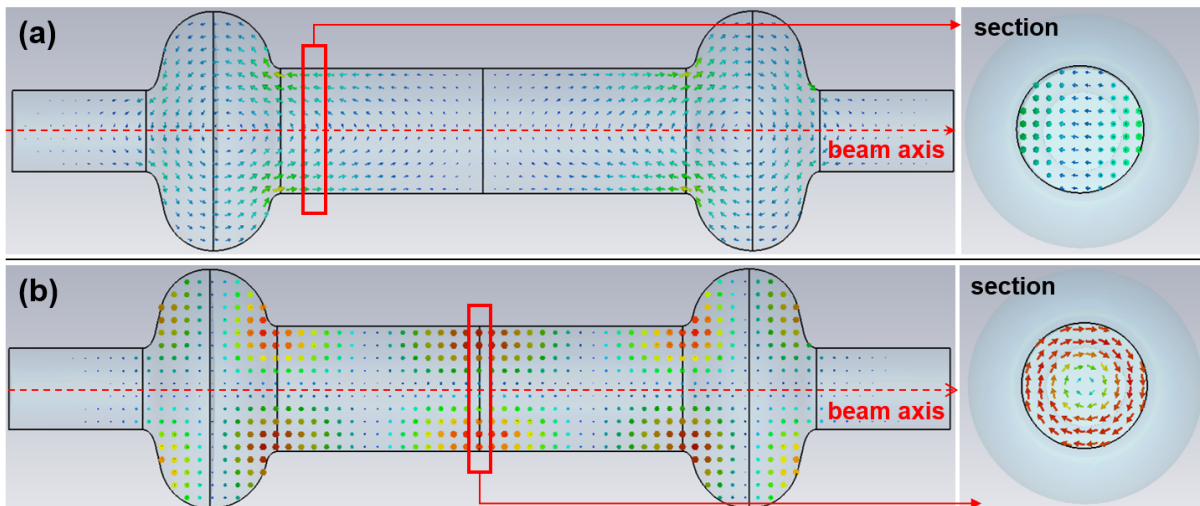


**Fig. 3.** HOMs magnetic field distribution, (a)  $TE_{112}$  distribution, (b)  $TM_{015}$  distribution.

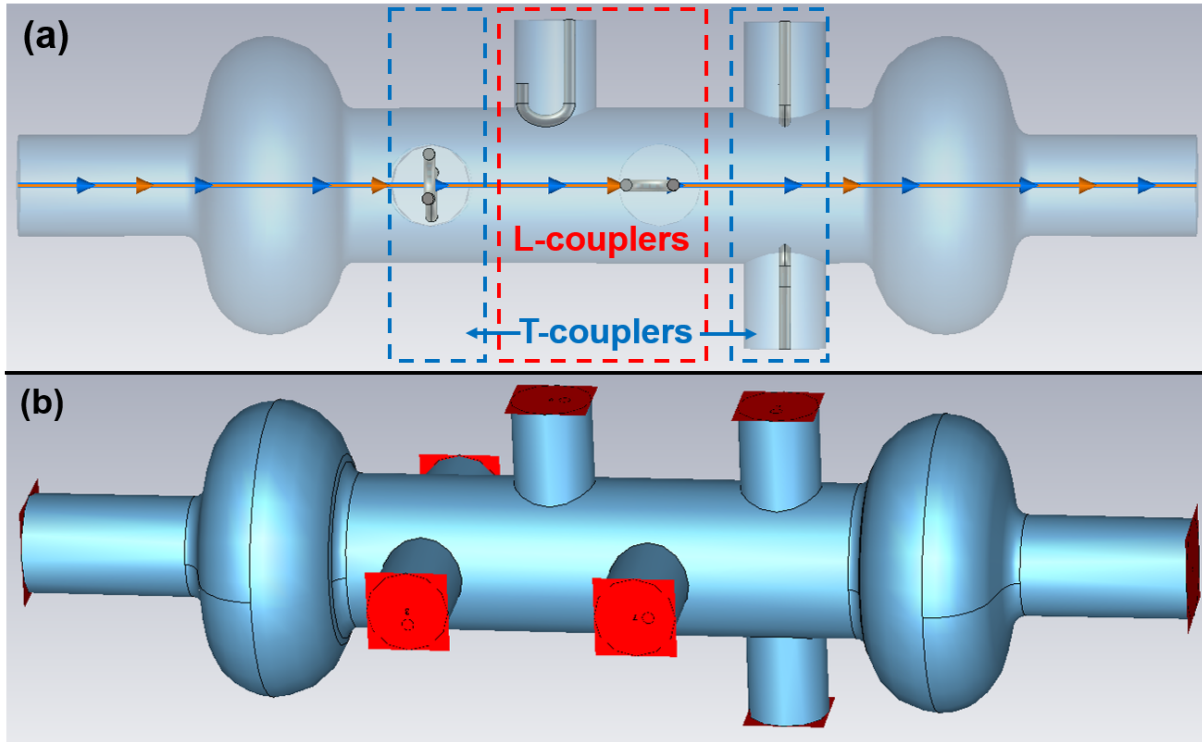


Fig. 4. Cavity model with the coupling hooks, (a) the hooks, (b) the port setting.

beam length of 34 mm was chosen to calculate the impedance accurately. Finally, 4 T-type couplers were symmetrically localized 137.5 mm from the cells and rotated 90 degrees on one side. At least 2 L-type couplers should be located around the center, as shown in Fig. 4, 362.5 mm from the cells.

The wake impedance results for the optimized model are shown in Fig. 5. The red lines are the impedance thresholds calculated by Eqs. (1) and (2) with the HALF parameters. The longitudinal impedance was well suppressed, and the maximum transverse impedance remained approximately 20 kΩ/m below the threshold. In this phase, a negative effect on the transverse impedance caused by the asymmetry of the L-type couplers was discovered but was considered acceptable for reducing the number of couplers.

### 3 RF design of HOM couplers

The coaxial line does not have the same cutoff property as the wakeguide, so coaxial HOM couplers need a filter structure at the fundamental mode frequency to prevent coupling of the fundamental mode, which in our case is 499.8 MHz. Filter structures can be realized by folding coaxial lines or adding extra rods or plates<sup>[14,15]</sup>. The optimized equivalent circuits and models of our L-type and T-type couplers are shown in Fig. 6.

Both couplers have one filter structure: a capacitor plate around the support rod for L-type couplers and a lengthened hook facing the outer conductor for T-type couplers, as shown in the red boxes of Fig. 6a and b, respectively. Since T-type couplers are close to the cavity cell, a filter structure around the coupler hook may block the fundamental mode from entering the coupler, reducing extra heat loss. In the L-

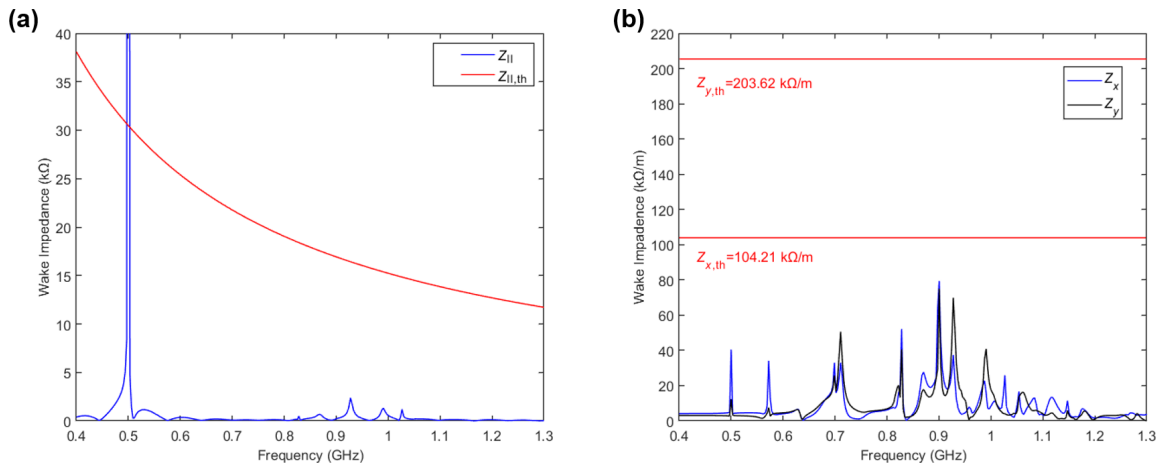


Fig. 5. Wake impedance of the optimized model: (a) longitudinal and (b) transverse.

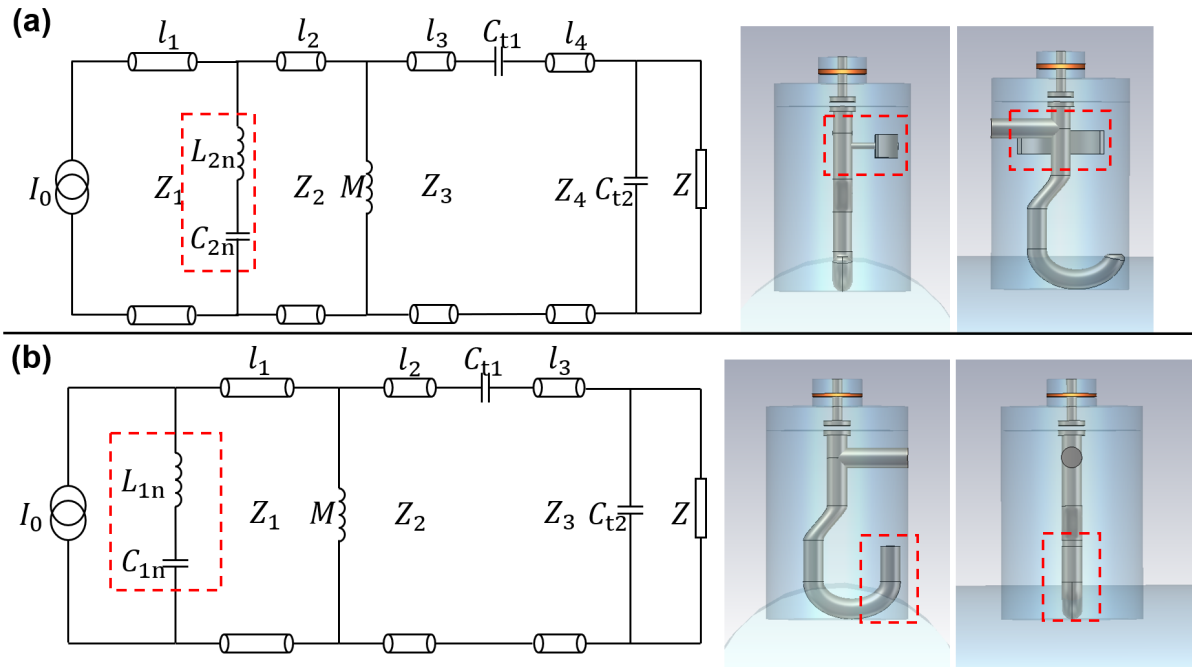


Fig. 6. Equivalent circuits and the optimized modal, (a) L-type coupler, (b) T-type coupler.

type coupler case, the fundamental mode fields were weak around the coupler, and the lengthened hook did not work as a filter after 90 degrees of rotation, so the hook was shortened, and a capacitor plate was added around the support rod.

The transport properties of these couplers were analyzed by beampipe-coupler models using CST microwave (MW) studio. As shown in the left part of Fig. 7, the  $TE_{11}$  or  $TM_{01}$  mode was launched at the side of the beam pipe, where it was set as a waveguide port named port1 or port3. Port2 was set to the TEM mode. The  $S_{21}$  results are shown in the right part of Fig. 7. Since the fundamental mode  $TM_{010}$  excites the  $TM_{01}$  mode at the beam pipe port, the  $TM_{01}$  mode  $S_{21}$  should receive special attention. After the optimization of the coupler geometry, both couplers exhibited good reflection properties—over  $-80$  dB for L-type couplers and  $-75$  dB for T-type couplers—at 499.8 MHz.

Longitudinal HOMs were extracted from L-type couplers. As shown by the blue line in Fig. 2, the longitudinal HOMs were located between 0.80 GHz and 1.26 GHz, with the strongest occurring at approximately 1.00 GHz. The  $TM_{01}$  launched  $S_{21}$  for the L-type coupler in this range was mostly above  $-20$  dB, which predicted good transmission. On the other hand, the transverse HOMs were located between 0.55 GHz and 1.10 GHz, and the T-type couplers also exhibited good transmission properties in two polarization directions.

#### 4 Multipacting analysis of HOM couplers

Multipacting (MP) is a phenomenon caused by electrons that resonate with electromagnetic fields. When some primary electrons gain energy from the field and collide with conductors, secondary electrons may be generated. If secondary electrons act similar to primary electrons and form more secondary electrons, the number of electrons will increase exponentially, and then the MP will occur. MP results in extra heat loss, quench of the superconducting, or even breakdown of

HOM couplers.

The particle in cell (PIC) solver in CST particle studio was used for MP analysis because it has several advantages, such as convenient particle settings and better computer memory processing compared with the tracking solver, while maintaining comparable accuracy<sup>[16]</sup>. The electromagnetic field was calculated by a model including the cavity and HOM couplers using the eigenmode solver of CST MW Studio and then input into the PIC solver. The model and electromagnetic field are presented in Fig. 8. Since the fundamental mode is below the cutoff frequency of the CBP, fields were localized inside cavity cells. The brown parts in Fig. 8 were alumina ceramics.

When the cavity is in operation, the electromagnetic field in the HOM couplers could be as strong as the field in cavity cells. Thus, niobium was chosen as the material for the inner conductor of HOM couplers, enabling the formation of a superconductive state, as illustrated in the blue parts of Fig. 9a.

In the PIC solver, the Furman emission model was used to simulate the MP effect. The backscattered electrons, redifused electrons and trun electrons were all considered in this model. A niobium shell must be added outside the cavity to make the cavity boundary reflectable, as shown in Fig. 9a. The secondary emission yield (SEY) of niobium and copper was obtained from the offset in the CST particle studio, as shown in Fig. 9b.

##### 4.1 T-type coupler multipacting analysis

Close to the cavity, the T-type couplers were analyzed first. All the inner conductor surfaces were set as particle sources, as shown in Fig. 10a. Over 2000 primary electron launch points were uniformly distributed on the surface. The electron launch angle was set to a random range from  $0^\circ$  to  $89.9^\circ$  with an initial energy of 2 eV. In the time domain, the launch current was set as a 2 ns rectangular pulse, covering the first period of the fundamental mode resonance. Each calculation

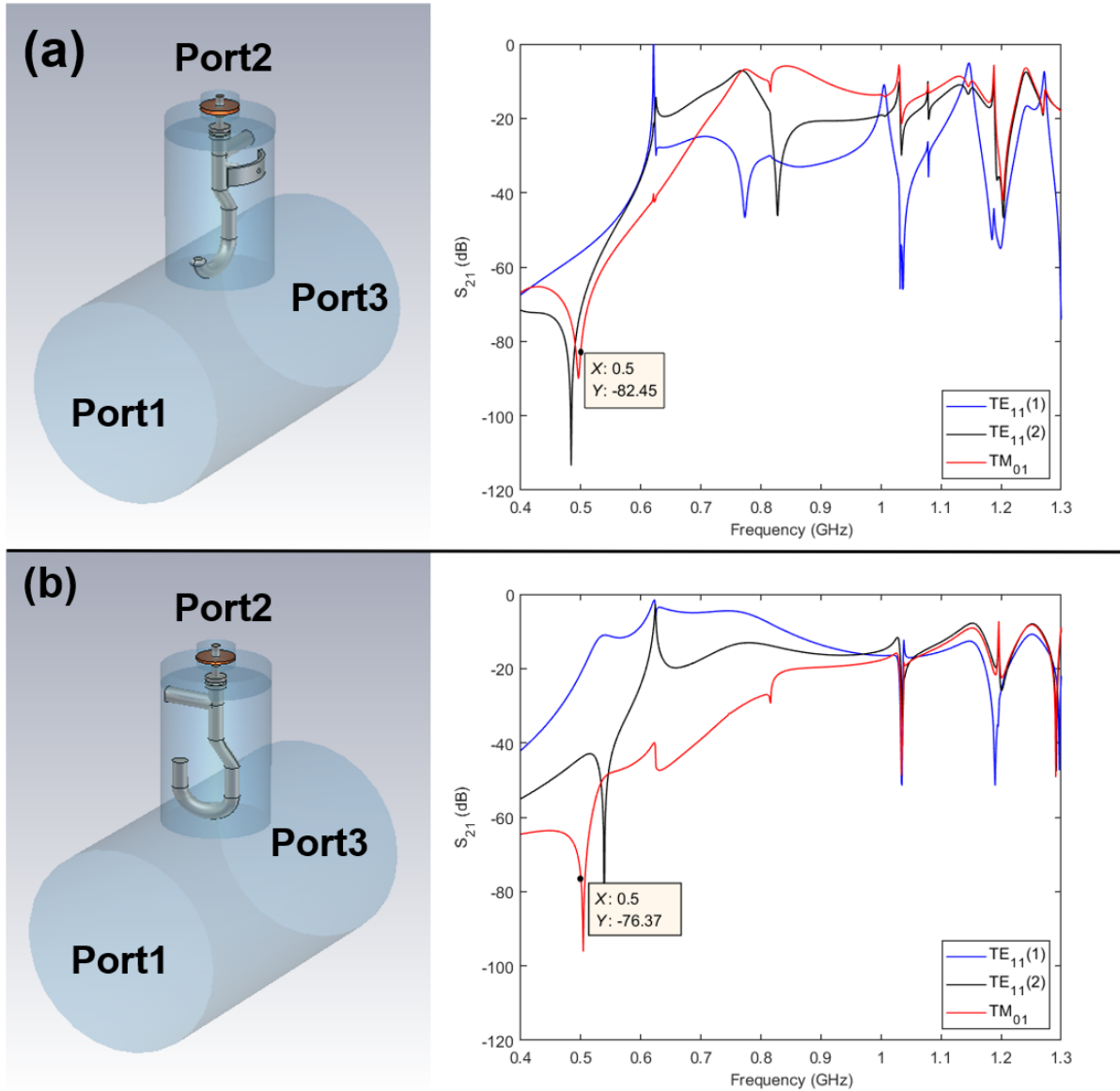


Fig. 7. Beampipe-coupler models and S21 results for the (a) L-type coupler and (b) T-type coupler.

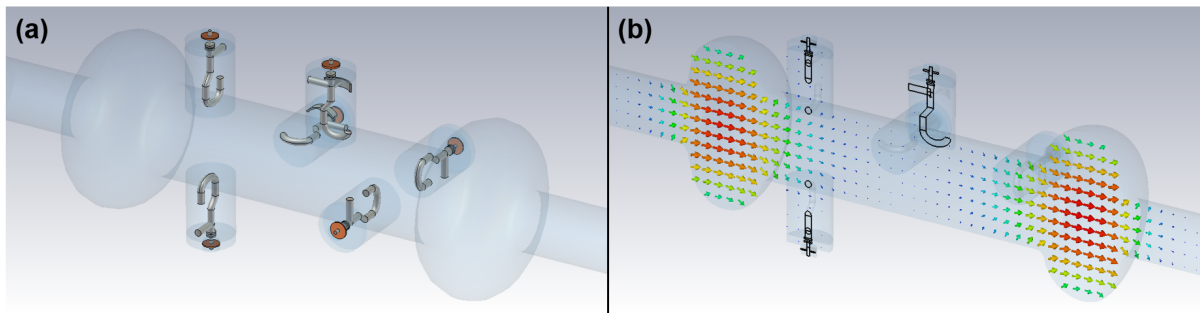


Fig. 8. Electromagnetic field model, (a) cavity model with couplers, (b) fundamental mode electric field.

was run for 15 ns, and the space-charge effect was neglected.

The time-averaged secondary emission yield ( $\langle SEY \rangle$ ) was used to indicate whether MP occurred, and it could be calculated by Eq. (3):

$$\langle SEY \rangle = \frac{\langle I_e \rangle}{\langle I_c \rangle}, \quad (3)$$

$\langle I_e \rangle$  and  $\langle I_c \rangle$  represent the time-averaged emission current and collision current, respectively, calculated by electrons emitted from or colliding with the entire conductor surface and averaged from the simulation time of 4 ns to 15 ns. When  $\langle SEY \rangle$  is greater than 1, the emission current is greater than the collision current, which always represents a high possibil-

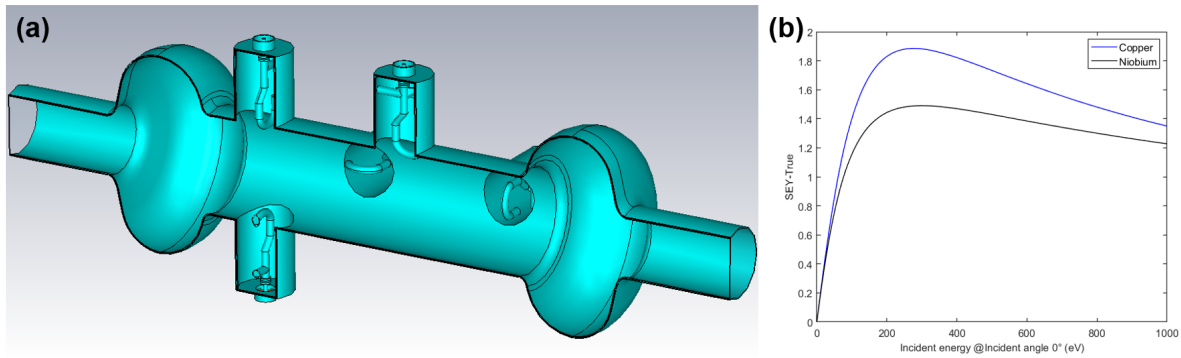


Fig. 9. MP analysis model and true SEY used: (a) model and (b) SEY curve

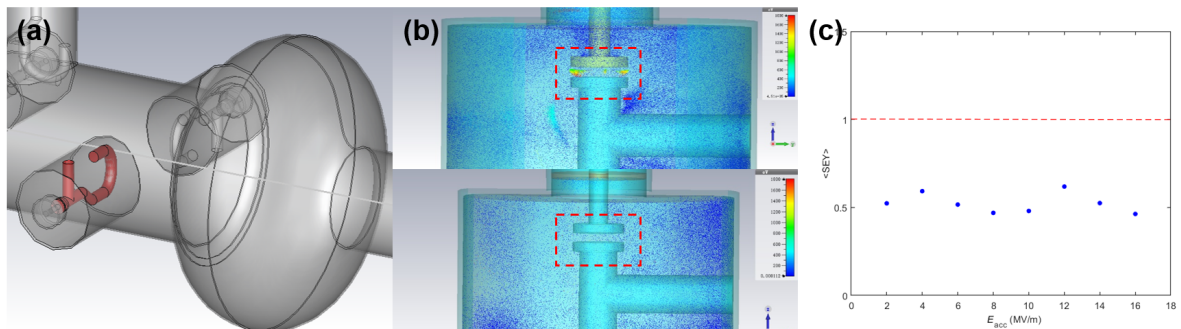


Fig. 10. MP analysis for T-type couplers: (a) particle source area, (b) particle monitoring where MPs occurred, and (c)  $\langle SEY \rangle$  results.

ity that MP may occur.

Initially, the materials of the upper coaxial line and the hook were set as copper and niobium, respectively, but MP occurred at an acceleration gradient of approximately 4 MV/m. Particle monitor revealed that the MP was located at the capacity part, as shown in the upper panel of Fig. 10b. After the upper part was replaced by niobium, the MP was suppressed well between the 2 MV/m and 16 MV/m acceleration gradients.

#### 4.2 L-type coupler multipacting analysis

Contrary to what we predicted, L-type couplers have a weak field strength inside but are more likely to experience MP. Similar to T-type couplers, the entire inner conductor surface was set as a particle source, as shown in Fig. 11a. All primary electron settings and the  $\langle SEY \rangle$  calculations were consistent with the T-type coupler analysis.

After optimization, MP still occurred over 10 MV/m at the capacity plate facing the outer conductor, as shown in the up-

per panel of Fig. 11b. An inner conductor capacity plate might also lead to an MP under a higher acceleration gradient. As a storage ring cavity, the acceleration gradient was always set between 2 MV/m and 6 MV/m, rarely more than 8 MV/m. In this range, optimized L-type couplers had a low probability of having an MP effect. The HALF required a 1.5 MV RF voltage, and the acceleration gradient could be calculated to be 2.48 MV/m per cell using a 499.8 MHz SOLEIL-type cavity. It could be predicted that no multipacting will occur under an operating acceleration gradient in L-type or T-type HOM couplers.

### 5 Results and discussion

#### 5.1 Wake impedance recalculation

After RF and MP analysis, the structure of HOM couplers is finally determined. To ensure that these couplers could dampen HOMs efficiently, the wake impedance was recalculated.

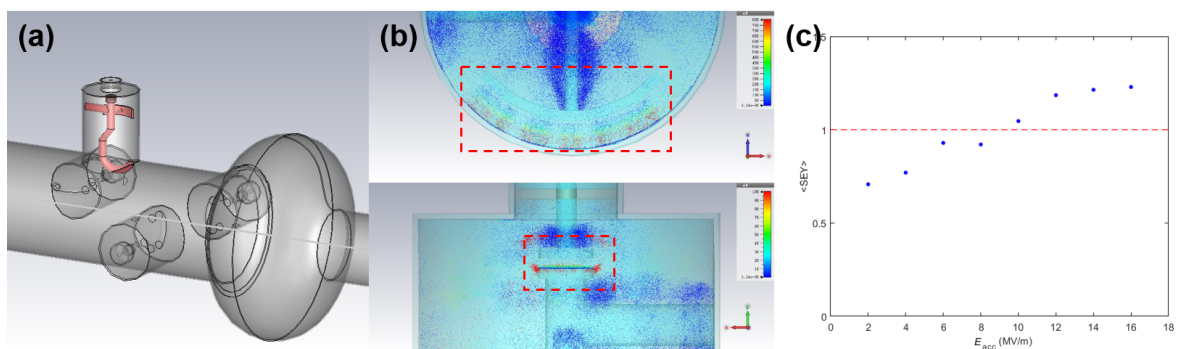
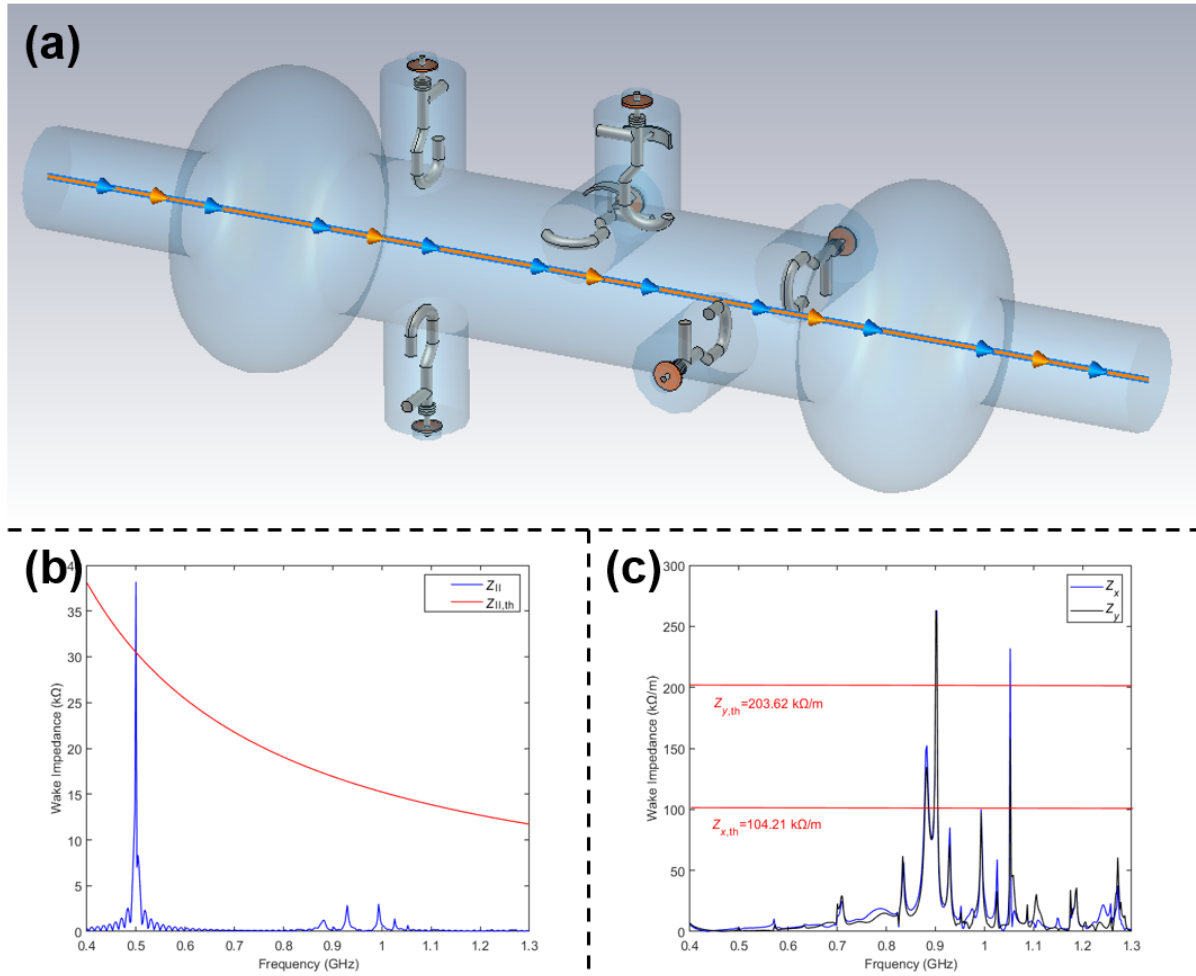


Fig. 11. MP analysis for L-type couplers: (a) particle source area, (b) particle monitoring where MPs occurred, and (c)  $\langle SEY \rangle$  results





**Fig. 12.** The cavity model and its impedances: (a) model with 4 T-type and 2 L-type couplers, (b) longitudinal impedance, (c) transverse impedance

lated with a model including detailed HOM couplers and the cavity, as shown in Fig. 12a.

In this model, the coupling hooks were replaced by 4 T-type couplers and 2 L-type couplers in detail. The beam length was set to 50 mm after a tradeoff between accuracy and calculation time, and the beam position was set to 1 mm biased from the beam axis. To ensure that all the HOMs with frequencies less than 1.3 GHz could be extracted, two SBP ports were set as waveguide ports with five modes, and all the HOM coupler ports were set as waveguide ports with three modes. The impedance results are presented in Fig. 12b and c, and the longitudinal impedances were well damped. Unfortunately, the transverse impedance greatly exceeds the threshold.

To ensure that the transverse impedance is below the threshold, the asymmetry effect of L-type couplers was considered. Two extra L-type couplers were added opposite to the former L-type couplers shown in Fig. 13a, all of which are located 362.5 mm from the cavity. During the calculations, all beam parameter settings were inherited from the previous model. The addition of two L-type couplers resulted in a significant reduction in both longitudinal and transverse impedance, as shown in Fig. 13b and c.

## 5.2 Thermal analysis

Finally, a preliminary thermal analysis of HOM couplers was performed. Using CST Microwave Studio and Mphsics Studio, a bi-directional electromagnetic-thermal calculation was studied. The model is presented in Fig. 14a. Since the cells of the SOLEIL-type cavity were completely immersed in 4.2 K liquid helium and the CBP part was in vacuum. The cavity cells were assumed well cooled and simplified with two 4.2 K thermal anchors on both sides of the CBP<sup>[3,4]</sup>. T-type couplers were also assumed to be cooled by 4.2 K liquid helium because they were close to the cavity cell. Additionally, a 5 K thermal anchor was added at the top of each HOM coupler for thermal calculations. The 4.2 K and 5 K thermal anchors are shown in blue and red, respectively, in Fig. 14a. The thickness of the CBP niobium wall was 4 mm. The temperature-dependent heat conductivity and electrical conductivity of niobium were obtained from Fermilab documents<sup>[17]</sup>. The surface resistance of the superconductive niobium was set to 20 nΩ at 4.2 K and 1 GHz, with a residual resistance of 10 nΩ. This value exhibits variations with both temperature and frequency according to the following formula<sup>[2]</sup>:

$$R_s = A(1/T)f^2 \exp(-\Delta/kT) + R_0, \quad (4)$$

with A a constant factor, T is the temperature, f is the frequency, Δ is the half-energy gap of niobium, k is the Boltzmann constant and R<sub>0</sub> is the residual resistance. Other

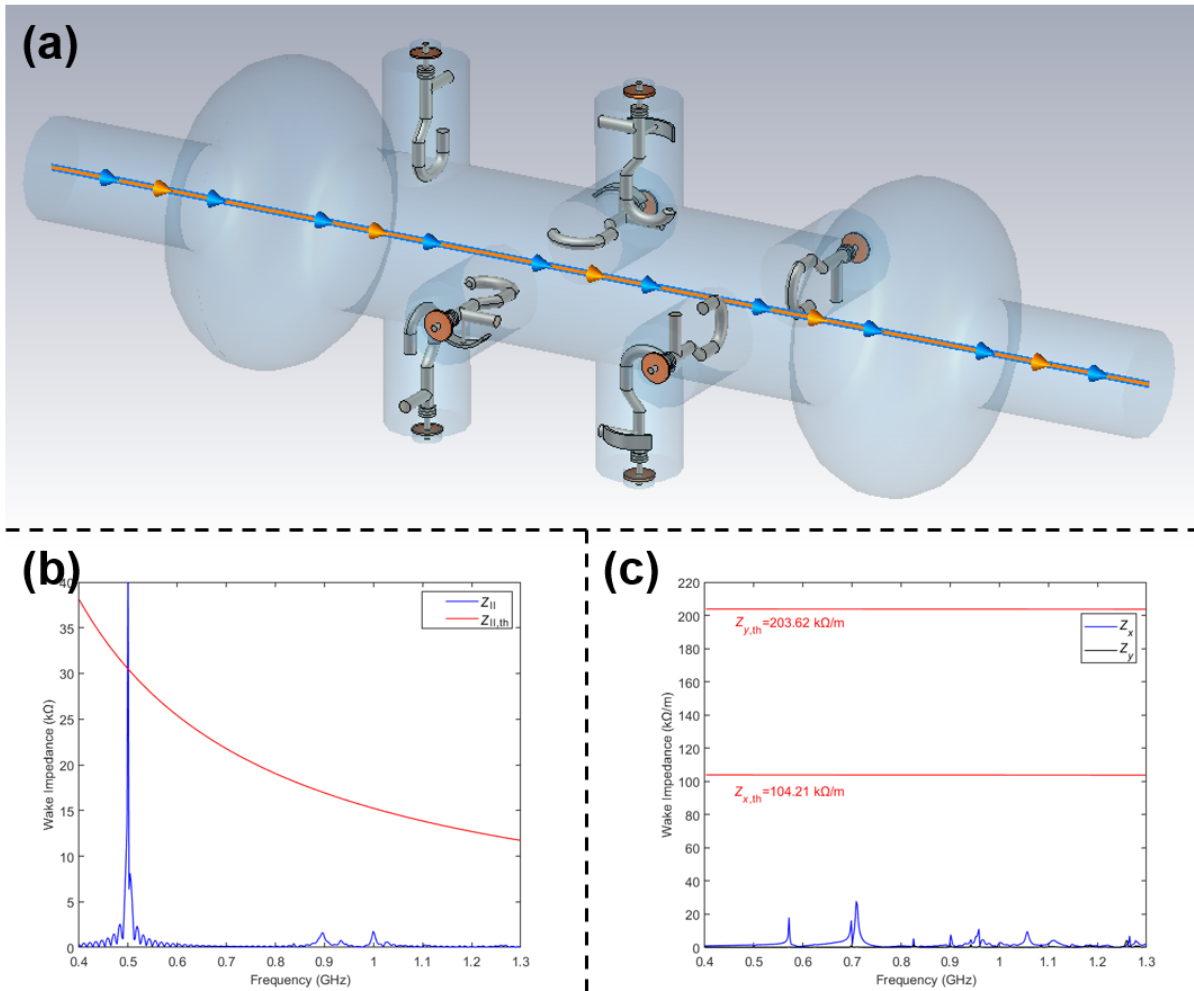


**Fig. 13.** The cavity model and its impedances: (a) model with 4 T-type and 4 L-type couplers, (b) longitudinal impedance, (c) transverse impedance

materials, such as ceramics, were obtained from the CST library as a default.

In this model, the  $TM_{01}$  mode waveguide ports on both sides of the CBP represented the power launched by the  $TM_{10}$  mode in the cavity cells, as shown in Fig. 14a. The initial temperature distribution was calculated without RF power and input into microwave studio. Thereafter, new temperature distribution was computed based on the RF losses derived from the initial distribution. This iterative process was repeated until stable results were achieved. Two simulation conditions are presented as follows.

Since MP may not appear until a 10 MV/m acceleration

gradient is reached, the electromagnetic fields were scaled to 10 MV/m at 499.8 MHz for thermal analysis first. As shown in Fig. 14b, the hook parts of all HOM couplers remained superconducting. The maximum temperature was 8.3 K at the ceram part of the T-type couplers. With such a small temperature increase, there should be no thermal breakdown until MP occurs.

The second condition was established to simulate the temperature distribution under an acceleration gradient of 3 MV/m, taking HOM power into account, assuming the module was in operation. The HOM power could be calculated by the loss factor:

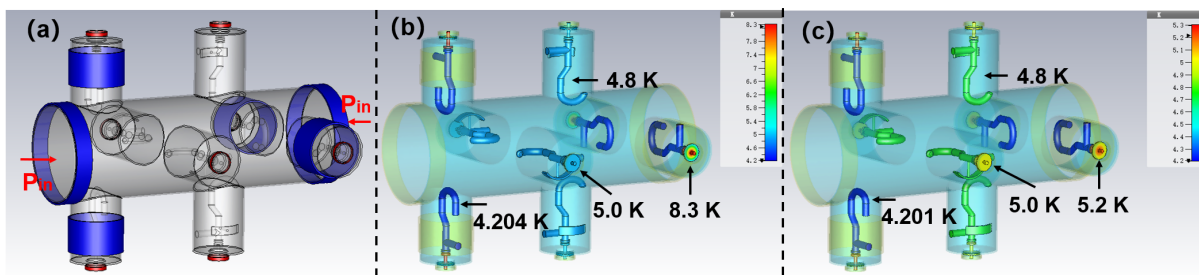


**Fig. 14.** Thermal analysis: (a) boundary conditions, (b) temperature distribution under a 10 MV/m acceleration gradient, and (c) temperature distribution under a 3 MV/m acceleration gradient and 2 kW HOM power

$$P_{\text{HOM}} = \frac{(k_{\parallel} - k_{\text{FM}})I_b^2}{Nf_{\text{rev}}}, \quad (5)$$

where  $k_{\parallel}$  is the total loss factor and  $k_{\text{FM}}$  is the loss factor for the fundamental mode.  $I_b$  is the beam current,  $N$  is the number of bunches and  $f_{\text{rev}}$  is the revolution frequency. The loss factor for the fundamental mode  $k_{\text{FM}}$  can be calculated by Eq. (6).

$$k_{\text{FM}} = \frac{\omega_{\text{FM}}}{4} \left( \frac{R}{Q} \right)_{\text{FM}} \exp\left(-\frac{\omega_{\text{FM}}^2 \sigma_z^2}{c^2}\right) \quad (6)$$

where  $\omega_{\text{FM}}$  and  $(R/Q)_{\text{FM}}$  is the angular frequency and the  $R$  over  $Q$  value of the fundamental mode,  $\sigma_z$  is the longitudinal beam length and  $c$  is the speed of light.

Using the model shown in Fig. 1, when the beam length was 5 mm, the total loss factor and the fundamental mode loss factor was computed to be 0.6 V/pC and 0.14 V/pC, respectively. With the parameters of HALF, the HOM power could be predicted to be less than 1 kW. However, the tapers and beam pipe HOM absorbers outside the model were proven to be important contributors to losses at short beam lengths<sup>[18]</sup>. Consequently, we assumed a total HOM power of 2 kW. On each side of the CBP, the 499.8 MHz and 1 GHz fields were scaled to fit a 3 MV/m gradient and 1 kW HOM power, respectively. The simulation results are shown in Fig. 14c. The maximum temperature was 5.2 K. The temperature distribution of the L-type couplers was nearly identical to that of under 10 MV/m gradient. While the T-type couplers had a lower temperature related to the decrease in the acceleration gradient. As a summary, the HOM power has minor influence on the temperature distribution. There are no risks of thermal breakdown under this condition.

## 6 Conclusions

SOLEIL-type superconducting cavities have two fundamental power couplers, which may easily provide a higher power level. Two kinds of coaxial HOM couplers were designed for a 499.8 MHz SOLEIL-type superconducting cavity. The geometry, quantity and location of these couplers were optimized. The RF transfer characteristics and MP properties were good until 10 MV/m was achieved. The HOM damping requirement of HALF can be greatly satisfied using 4 L-type and 4 T-type couplers. A preliminary thermal analysis showed that there should be no thermal breakdown until MPs occur. This work will provide preliminary research for a 499.8 MHz SOLEIL-type superconducting cavity.

## Acknowledgements

This work was supported by the Fundamental Research Funds for the Central Universities (WK2310000098).

## Conflict of interest

The authors declare that they have no conflict of interest.

## Biographies

**Xiyuan Chai** is currently a graduate student at the National Synchro-

tron Radiation Laboratory, University of Science and Technology of China, under the supervision of Associate Professor Cong-Feng Wu and Professor Duohui He. His research mainly focuses on superconducting radio frequency cavities for accelerators.

**Cong-Feng Wu** is currently an Associate Professor at National Synchrotron Radiation Laboratory, University of Science and Technology of China. She received her Ph.D. degree from Chinese Academy of Sciences Institute of Plasma Physics in 1999. Her research mainly focuses on superconducting radio frequency cavity system, microwave accelerating structure, and radio frequency plasma application.

## References

- [1] Padamsee H. 50 years of success for SRF accelerators—a review. *Superconductor Science and Technology*, **2017**, *30*: 053003.
- [2] Padamsee H, Knobloch J, Hays T, et al. RF superconductivity for accelerators. *Physics Today*, **1999**, *52*: 54.
- [3] Mosnier A, Chel S, Hanus X, et al. Design of a heavily damped superconducting cavity for SOLEIL. In: Proceedings of the 1997 Particle Accelerator Conference (Cat. No. 97CH36167). Vancouver, BC, Canada: IEEE, **1997**: 1709–1711.
- [4] Marchand P, Baete J P, Cuoq R, et al. Operational experience with the SOLEIL superconducting RF system. In: 16th International Conference on Radio-Frequency Superconductivity, **2013**, *MOP064*: 269–273.
- [5] Nadolski L S, Abeillé G, Abiven Y -M, et al. SOLEIL status report. In: 9th International Particle Accelerator Conference, **2018**, *THPMK092*: 4516–4519.
- [6] Furuya T, Asano K, Ishi Y, et al. Superconducting accelerating cavity for KEK B-factory. In: Proceedings of the 1995 Workshop on RF Superconductivity. Gif-sur-Yvette, France: JACoW Publishing, **1995**: 729–733.
- [7] Huang T, Pan W, Wang G, et al. The development of the 499.8MHz superconducting cavity system for BEPCII. *Nuclear Instruments and Methods in Physics Research Section A: Accelerators, Spectrometers, Detectors and Associated Equipment*, **2021**, *1013*: 165649.
- [8] Wu C F, Tang Y, Tan M, et al. Research of the 499.8 MHz superconducting cavity system for HALF. *Nuclear Instruments and Methods in Physics Research Section A: Accelerators, Spectrometers, Detectors and Associated Equipment*, **2023**, *1050*: 168176.
- [9] Marhauser F. Next generation HOM-damping. *Superconductor Science and Technology*, **2017**, *30*: 063002.
- [10] Craievich P, Bosland P, Chel S, et al. HOM couplers design for the SUPER-3HC cavity. In: PACS2001. Proceedings of the 2001 Particle Accelerator Conference (Cat. No. 01CH37268). Chicago, IL, USA: IEEE, **2001**: 1134–1136.
- [11] Rimmer R A, Byrd J M, Li D. Comparison of calculated, measured, and beam sampled impedances of a higher-order-mode-damped rf cavity. *Physical Review Special Topics Accelerators and Beams*, **2000**, *3*: 102001.
- [12] Rimmer R A. Higher-order mode calculations, predictions and overview of damping schemes for energy recovering linacs. *Nuclear Instruments and Methods in Physics Research Section A: Accelerators, Spectrometers, Detectors and Associated Equipment*, **2006**, *557*: 259–267.
- [13] Haeibel E. Couplers for cavities. In: *CAS - CERN Accelerator School: Superconductivity in Particle Accelerators*, **1996**: 231–264.
- [14] Sekutowicz J. Higher order mode coupler for TESLA. In: Proceedings of the Sixth Workshop on RF Superconductivity, Virginia, USA: CEBAF, Newport News, **1993**, 426–439.
- [15] Papke K, Gerigk F, van Rienen U. Comparison of coaxial higher order mode couplers for the CERN Superconducting Proton Linac study. *Physical Review Accelerators and Beams*, **2017**, *20*: 060401.
- [16] Romanov G, Berrutti P, Khabiboulline T. Simulation of multipacting in SC low beta cavities at FNAL. In: 6th International Particle Accelerator Conference, Richmond, VA, USA: JACoW Publishing, **2015**: 579–581.
- [17] Merio M. Material Properties for Engineering Analysis of SRF Cavities. Batavia, Illinois, USA: FermiLab, **2011**, Fermilab Specification 5500.000-ES-371110.
- [18] Yu H, Liu J, Hou H, et al. Simulation of higher order modes and loss factor of a new type of 500-MHz single cell superconducting cavity at SSRF. *Nuclear Science and Techniques*, **2011**, *22* (5) : 257–260.